SEED METERING PERFORMANCE DETECTION SYSTEM BASED ON OPTIC FIBER SENSOR

Yin CHEN[11], Kexin XU[2], Jianqiao WANG[3], Tianhao JING[4], Yulong CHEN[5*], Meng ZHANG[6]

Accurate detection of seed metering performance is essential for achieving precise seed distribution. While photoelectric sensors and machine vision technologies are widely used for this purpose, they face limitations such as susceptibility to interference and high costs. This study employed a through-beam fiber-optic sensor to monitor seed flow, which generated continuous pulse signals during operation. An ICAN7404 module coupled with an STM32 microcontroller processed these signals to evaluate seed metering performance, while a human-computer interaction module dynamically displayed detection parameters. The research developed integrated hardware and software components for the system and experimentally validated its seed detection capabilities. Results demonstrate that the intelligent variable-rate precision seed metering detection system achieves accurate performance monitoring, with both component-level and system-level metrics meeting precision seeding operational requirements. The proposed framework and findings provide novel insights for advancing intelligent seed metering systems.

Keywords: seed metering system; through-beam fiber-optic sensor; CANopen protocol

1. Introduction

Intelligent variable-rate technology in agricultural machinery has emerged as a key research and application area in developed countries [1-4]. Extensive experimental studies have been conducted, leading to the development of advanced intelligent precision seeding automation control systems [5-8]. Detection devices in

[1] College of Agricultural Engineering and Food Science, Institute of Modern Agricultural Equipment, Shandong University of Technology, Zibo, 255000, China, e-mail: 2874194730@qq.com

[2]College of Agricultural Engineering and Food Science, Shandong University of Technology Zibo, 255000, China, e-mail: 2536570601@qq.com

[3]College of Agricultural Engineering and Food Science, Shandong University of Technology, Zibo, 255000, China, e-mail: 19811709920@163.com

[4]College of Agricultural Engineering and Food Science, Shandong University of Technology, Zibo, 255000, China, e-mail: 18353169398@163.com

[5*]College of Agricultural Engineering and Food Science, Institute of Modern Agricultural Equipment, Shandong University of Technology, Zibo, 255000, China, e-mail: cyl06471@sdut.edu.cn (corresponding author)

[6]Weichai Leiwo Intelligent Agriculture Technology Co, Weifang, 261206, China, e-mail: 411225919@qq.com

precision seeders can be classified into three categories according to their operational principles: mechanical, electromechanical, and electronic. The monitoring system displays reseeding rate, missed seeding rate, seeding spacing, seeding area, and seeding quantity, significantly reducing issues such as missed seeding [9-11]. The detection system uses light and sound sensors to monitor seed metering, ensuring seeding uniformity. MICRO-TRAK's electronic device measures speed, area, spacing, and change speed, while John Deere's SeedStarTMXP enhances seeder control [12-14], employs CAN communication with distributed multi-controller processing, enabling seeding spacing detection, real-time seeding rate, downforce control, and fertilizer pressure management, etc [15-17]. Jia Honglei et al. designed a photoelectric sensor-based seed suction detection system, with field tests showing the missed seeding rate was 3.87% and reseeding rate was 8.42%. Cao Ye developed a seeding performance detection system based on machine vision for hole seeders [18-19]. Test results revealed a 2.7% detection error for qualified seeding rate, validating system feasibility. The relative errors of the seeding detection system for wheat based on capacitor ranged from -2.26% to 2.17%. Ding Youchun et al. designed a seeding detection system based on piezoelectric film for rape precision seeders [20-22]. Bench and field tests demonstrated more than 96% seeding detection accuracy with a 60 m wireless transmission range. Ji Chao et al. developed a reflective system based on infrared photoelectric sensor system achieving 98.5% seeding detection accuracy, while its self-cleaning mechanism maintained 98.1% accuracy under dust conditions. Yang Shuo et al. designed an online grain spacing detection system for corn precision seeders based on infrared beam sensor [23-24]. Field tests revealed seeding spacing detection errors of 1.84 cm and 2.22 cm at 5.49 $km \cdot h^{-1}$ and 8.49 $km \cdot h^{-1}$, respectively, with a target spacing of 25 cm.

Recent advances in intelligent variable speed agricultural machinery have integrated a multi-sensor fusion architecture to enable real-time accurate seed variable monitoring. Experimental validation under controlled laboratory conditions showed a seed detection accuracy of 96%. However, performance degradation was observed in high-speed operations and unstructured field environments with spatially varying soil texture and terrain irregularities. In this paper, we propose a novel electromechanical optimization framework that addresses these limitations, incorporating sensor layout redesign, adaptive noise filtering algorithms, and inertia compensation mechanisms.

2.Materials and Methods

2.1 Hardware selection of seed metering performance testing system

The length, width and thickness of 100 corn seeds were measured randomly. The length of the seeds ranged from 11.15 mm to 12.87 mm with an average of

12.08 mm; the width ranged from 7.64 mm to 9.83 mm with an average of 8.91 mm; and the thickness ranged from 4.28 mm to 6.08 mm with an average of 5.25 mm. Fig. 1 illustrates that the length, width, and thickness of the measured maize seeds all follow an approximately normal distribution. The seed monitoring sensor was installed 30 cm below the seeding point. The time corn seed drop through the sensor varied between 1.74 ms and 5.23 ms, at 12 km·h^{-1}. Therefore, the minimum response time of the selected seed monitoring sensor is less than 1.74 ms, while the minimum detection object of the sensor is less than 4.28 mm.

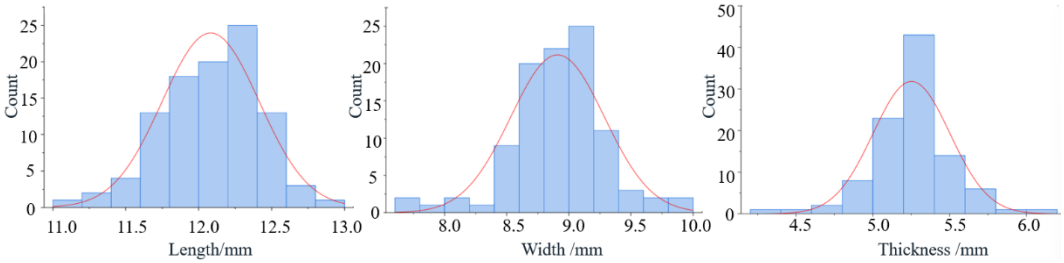

Fig.1 Distribution of the triaxial dimensions of maize seeds

As shown in Fig. 2, the through-beam fiber-optic sensor (TBFOS) is located 220 mm below the uppermost point of the seed guide tube entrance, which has an opposite dimension of 37 mm and a lateral dimension of 20 mm. The TBFOS requires an opposite detection distance of more than 30 mm and a lateral detection distance of more than 20 mm.

The seed metering detection system integrated the TBFOS with an amplification module. A detailed introduction is provided for the PT30QL sensor employing NPN output and its ER2-18ZW amplifier. Operating at 12 - 24V DC, the sensor demonstrates a current consumption below 30 mA and achieves a response latency of 500 μs.

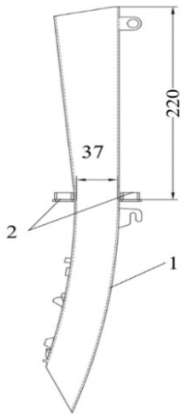

Fig.2 Section size of sensor installation. 1.seed guide tube 2.TBFOS

The amplifier is configured with normally closed (NC) output, exhibiting opposite detection capability up to 700 μm and lateral coverage spanning 30 mm. The object to be detected by the amplifier requires to be larger than 2 mm.

The human-computer interaction module served dual functions: (1) the operator terminal enabled configuration of real-time seeding parameters (e.g., seeding spacing, number of suction holes on the seed metering plate) and execution of system start/stop control; (2) the monitoring interface dynamically displayed key operational parameters, including operating speed, seed metering plate rotational speed, seeding spacing, fan rotational speed, and fan negative pressure. Based on the communication distance between the human-computer interaction module and STM32 microcontroller should be controlled at 10 m, the system selected TJC8048X570 serial port touch screen as the interaction terminal. The hardware platform supported visualization interface design through the USART HMI software development environment.

2.2 Seed detection system based on optical fiber sensor

The amplifier utilized an NPN-type NC-open collector output configuration. A 10 kΩ pull-up resistor was used to boost the signal to 3.3 V to achieve compatibility with the system. The output was held low at 0 V when no seed was detected. The output transitions to a high-level of 3.3 V when a seed passed through the sensor. The duration of the high-level signal corresponded to the time it took for the seed to pass through the sensor. And the low-level duration indicated the time between the next seed being detected by the sensor. In each cycle of the continuous square wave, the sum of the high-level and low-level durations was equal to the time interval between two consecutive seeds passing through the sensor. This time interval was measured with an oscilloscope.

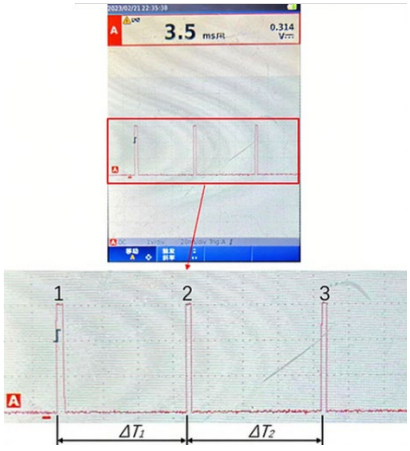

Fig.3 Output waveform of corn seeds through amplifier

As shown in Fig. 3, the high-level signals 1, 2, and 3 correspond to individual maize seeds passing through the detection zone, with each high-level pulse maintaining a duration of approximately 3.5 ms. This indicates that the transit time for maize seeds through the TBFOS detection area is 3.5 ms. ΔT_1 and ΔT_2 represent the time intervals between consecutive seed passages. Notably, these intervals are not equal (i.e., $\Delta T_1 \neq \Delta T_2$), which reflects the inherent variability in the seeding process. To verify the reliability of the detection sensor, maize seeds passing through the TBFOS were counted using the external interrupt function on the PB0 pin on the STM32 microcontroller. Then, the digital input pin EIN1 of the ICAN7404 module was employed to analyze the pulse output period from the amplifier via CAN communication. By integrating operational speed parameters, the seeding spacing was calculated using the formula presented in Equ.1, with the complete workflow detailed in Fig.4.

$$X_{r_i} = \Delta T_i \cdot V \tag{1}$$

Where : Xr_i is the i-th actual seeding spacing, cm;

ΔT_i is the i-th time between two consecutive seeds, s.

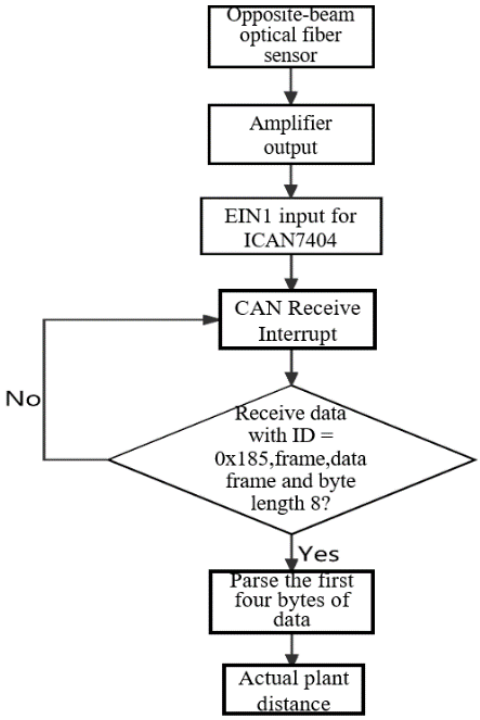

Fig.4 Calculate the seeding spacing process

The serial interface display transmits data to the STM32 microcontroller via the Tx serial communication interface in hexadecimal format. In order to recognize different data and judge whether the data transmission is finished or not, it is

necessary to define different header identifier and footer identifier when sending data, which mainly involves printh, prints and other instructions to facilitate parameter transmission. The serial interface display receives the data sent from the PA2 pin of the microcontroller through the serial communication interface in Rx. STM32 needs to send three consecutive 0xFF as the end-of-frame after sending the valid data. The system utilizes the built-in printf function of the microcontroller's serial port for efficient variable transmission.

2.3 Comprehensive performance test of seed metering system

The pneumatic seed meter of the vSet series from Precision Planting Company was selected. The seeding performance of the seed metering system was quantitatively evaluated using the image processing system integrated with the JPS-12 test bench. The TBFOS and the image processing system were utilized simultaneously to detect the performance of the seed metering system, aiming to investigate the seed metering detection performance of the TBFOS in comparison to the image processing system. To comprehensively assess the performance of the seed metering system, a bench test was conducted using Zhengdan 958 maize seeds as the test subject. The experimental setup is illustrated in Fig. 5.

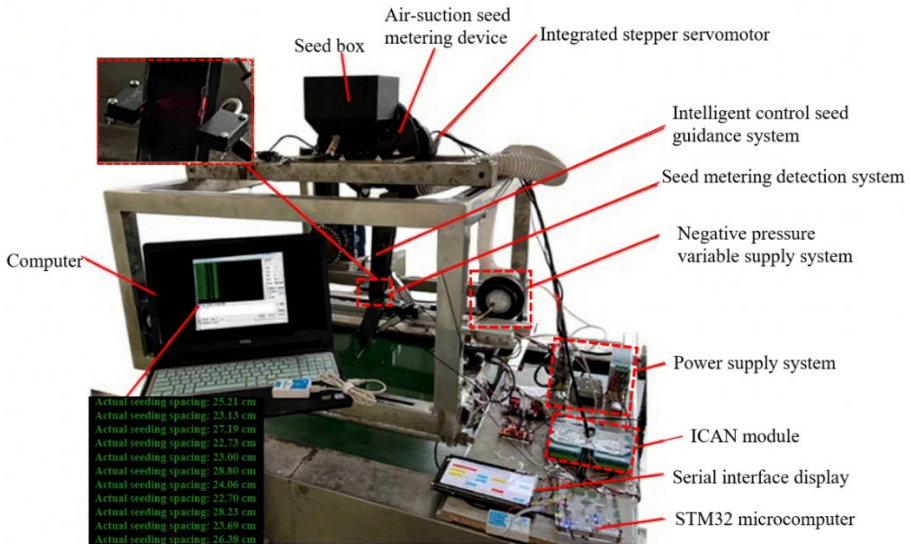

Fig.5 Seeding performance test bench.

The seeding performance was evaluated based on the following key performance indicators: qualified seeding rate (QSR), reseeding rate (RR), missed seeding rate (MSR), and coefficient of variation of seeding spacing (CVSS), coefficient of variation (CV), seeding spacing qualification rate (SSQR).

In accordance with the agronomic requirements for maize cultivation, the target seeding spacing Z for maize in this experiment was set at 25 cm [25]. A seeding spacing *Xr* within the range of 0.5 Z to 1.5 Z was classified as qualified. Seeding spacings less than 0.5 *Z* were categorized as reseeding, while those exceeding 1.5 *Z* were identified as missed seeding. The QSR, RR, MSR, CVSS were calculated using the following equations [26]:

$$A = \frac{n_1}{N} \times 100\% \tag{2}$$

$$D = \frac{n_2}{N} \times 100\% \tag{3}$$

$$M = \frac{n_3}{N} \times 100\% \tag{4}$$

$$C = \sqrt{\frac{\sum_{r=1}^{N}(X_r - \overline{X})^2}{N \cdot \overline{X}^2}} \times 100\% \tag{5}$$

where

N is the total number of measured seeding spacing;
n_1 is qualified number of seeding spacing;
n_2 is the number of reseed seeding spacing;
n_3 is the number of missed sowing seed distance;
A is the qualified seeding rate, %;
D is the reseeding rate, %;
M is the missed seeding rate, %;
C is the coefficient of variation of seeding spacing, %;
X_r is the actual seeding spacing, cm;
$\overline{X}$ is the seeding spacing, cm.

3.Experimental Results and Discussion

The TBFOS was used for seeding detection, with ICAN7404 module and microcontroller to calculate the seeding distance. The HMI displays the parameters and controlled operation. The reliability of the sensor was verified based on high-speed camera data.

3.1 Seeding performance test conclusion

A bench test was conducted to verify the detection accuracy of the sensor. The testing result is shown in Fig. 6. The seed metering system includes an air-suction seed metering device, an integrated stepper servo motor, a negative pressure fan, and a flexible seed guide tube.

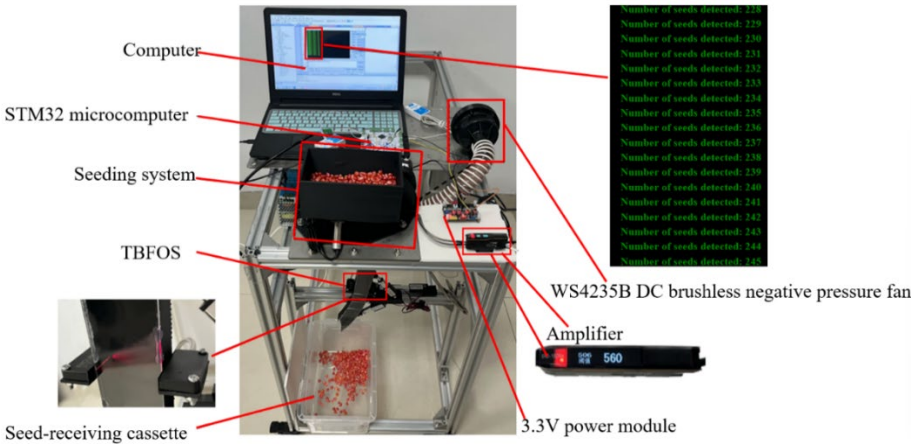

Fig.6 Seeding detection accuracy test bench.

At the operating speed of 2 - 12 km·h^{-1} and fan speed of 19,328.91 to 23,872.42 r·min^{-1}. The STM32 microcontroller timer, external interrupt and serial port were used to realize the counting of seeds detected in 1min. The detected values were output using the serial assistant. Three repetitions of the test were carried out under the same conditions and the actual values were counted manually as shown in Table 1. Values are presented as mean ± standard deviation.

Table 1

Average accuracy of seeding detection under different conditions

Operating speed, km·h^{-1}	Detection value	Real value	Average accuracy, %
2	143	143	99.29±0.72
	140	141	
	137	139	
4	271	275	98.07±1.53
	277	279	
	264	274	
6	407	412	98.71±0.14
	406	411	
	407	413	
8	547	552	99.09±0.54
	545	547	
	546	554	
10	680	684	99.12±0.51
	669	679	
	679	683	
12	805	816	98.53±0.21
	804	818	
	806	817	

As shown in Table 2, the average accuracy of the TBFOS detection was 98.84% at operating speeds between 2 and 12 km·h^{-1}. The detection accuracy showed high consistency across different operating speeds, with a low coefficient

of variation (CV) of 0.38%. The overall detection accuracy shows a trend of decreasing, then increasing and then decreasing with the increase of operating speed. At 12 km·h⁻¹, the detection accuracy still reaches 98.53%, so the sensor detection has high accuracy and high system stability.

At the operating speed of 2 - 12 km·h⁻¹, when the fan maintains the maximum speed, 251 seeds are continuously analyzed. Seeding spacing was detected by the TBFOS. These results were compared with those obtained from high-speed camera imaging.

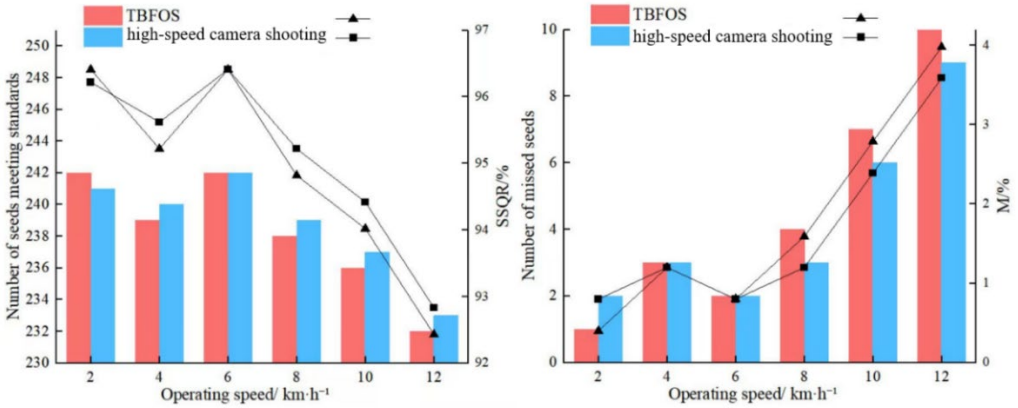

a. analysis of qualified seeds and SSQR at operating speed.

b. analysis of missed seeds and M at operating speeds.

Fig.7 Seeding performance comparison between TBFOS and high-speed camera detection

Comparative analysis of the TBFOS and high-speed camera shooting of seed performance detection effect, the results are shown in Fig. 7. When the operating speed is 2 - 8 km·h⁻¹, the A of the TBFOS and high-speed camera shooting seed spacing fluctuate in a similar pattern. When the operating speed was greater than 8 km·h⁻¹, the average value of seed spacing A under high-speed camera shooting increased slightly by 0.15% compared with that of the TBFOS. When the operating speed is 2 - 8 km·h⁻¹, the M for both the TBFOS and high-speed camera fluctuates around 1.08%. When more than 8 km·h⁻¹, the average value of the M of the TBFOS detection increases by 0.13% compared with that of high-speed camera shooting. Comprehensive analysis shows that the difference between the TBFOS and high-speed camera shooting of the A of seeding spacing and the average value of the M is less than 1%, so the TBFOS detection is stable and reliable.

3.2 Comparative detection methods results

The seeding performance of the seed metering device was systematically evaluated using both the JPS-12 test bench and the TBFOS at operating speeds of 2, 4, 6, 8, 10, and 12 km·h⁻¹. The corresponding results are illustrated in Fig. 8.

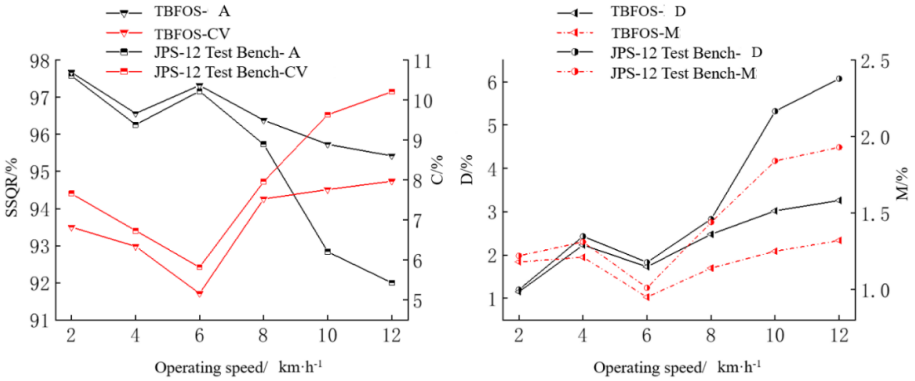

a. two methods for testing the A and CV of seeding spacing.

b. two methods for testing the D and M.

Fig.8 Performance comparison of different seeding detection systems

As shown in Fig. 8a, in the two testing methods, the A and the CCVS change in the same trend. When the speed is 2 - 8 km·h^{-1}, the average values of the A and the CV differ by 0.3% and 0.51% respectively. When the speed is 2 - 12 km·h^{-1}, compared with the JPS-12 test bench, the average values of the A and the CV detected by the TBFOS differ by 1.25% and 0.76% respectively. From Fig. 8b, when the speed is 2 - 8 km·h^{-1}, the average difference in the RR and M between the two testing methods was only 0.18% and 0.13%, respectively. When the speed is 2 - 12 km·h^{-1}, compared with the JPS-12 test bench, the average values of the RR and M detected by the TBFOS differ by 0.97% and 0.28% respectively.

At the operating speed of 2 - 12 km·h^{-1}, with acceleration times of 15, 30, and 45s, the seeding performance of the seeder was analyzed using the JPS-12 test bench and the TBFOS under variable speed conditions, as shown in Fig. 9.

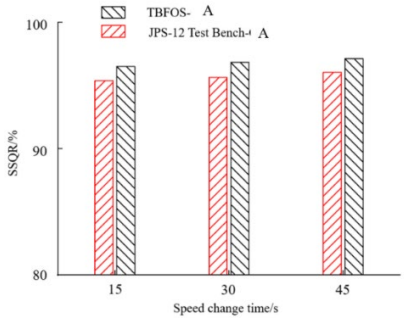

Fig.9 Variable-speed seeding spacing qualification rates between detection methods

As shown in Fig. 9, under variable speed conditions, the A measured by both methods remained high, with the TBFOS measurement being on average 1.13% higher than that of the JPS-12 test bench. Additionally, the TBFOS has a smaller error in detecting the seeding performance and is suitable for performance detection in different seeding systems.

4.Conclusions

(1) Comprehensive analysis was conducted on the three-dimensional dimensions of maize seeds, the installation distance of seed metering detection sensors below the seed drop point, and the positional dimensions within the seed guide tube. The PT30QL sensor and amplifier were selected as the core components for seed metering performance detection. A Taojingchi serial port screen was adopted as the human-machine interface (HMI) module to achieve multiple functions including real-time display of seed metering parameters, seeding data input, and start-stop control of the system. This integrated solution demonstrates effective implementation of precision seeding monitoring and control in agricultural machinery applications.

(2) The external interrupt function of the PB0 pin on the STM32 microcontroller was utilized to implement maize seed counting at the sensor detection point. Through the digital input pin EIN1 of the ICAN7404 module, combined with CAN interrupt processing, real-time parsing of the pulse signal frequency from the amplifier output was achieved. This frequency data was then integrated with operating speed parameters to calculate the actual seeding spacing through algorithmic processing.

(3) Bench test results demonstrated that within the operating speed range of 2 - 12 km·h^{-1}, the seeding accuracy detection maintained an average value of 98.84% with a CV of 0.38%. A 98.53% accuracy rate was still achieved at the maximum tested speed of 12 km·h^{-1}. Comparison and analysis of the sensor seeding detection performance with high-speed camera shooting, the difference between the average value of the seeding spacing A and M is less than 1%. The sensor demonstrates reliable adaptability across varying operating speeds for seed metering performance detection, owing to high measurement accuracy and operational stability.

(4) The average values of the TBFOS detect A, D, M and CV were 96.51%, 2.31%, 1.18%, and 6.93% at 2 - 12 km·h-1 operating speeds. These measurements showed deviations from the JPS-12 test bench, with differences of 1.25%, 0.97%, 0.28%, and 0.76% respectively. During change speed tests at 15, 30, and 45s intervals, the TBFOS system maintained an average SSQR of 96.81%, representing a 1.13 % improvement compared to the JPS-12 test bench. The results indicate that the TBFOS system exhibits minimal detection errors, high precision, and reliable performance in seed metering evaluation, demonstrating potential applicability for performance testing across different seed metering systems.

REFERENCES

[1] *Xie C ,Yang L ,He X , et al*. Maize precision seeding scheme based on multi-sensor information fusion[J].Journal of Industrial Information Integration,2025,**43**:100758-100758.

[2] *Lu J ,Liu S ,Wang Q , et al*. Research on Device and Sensing Technology for Precision Seeding of Potato[J].Agriculture,2024,**14**(12):2146-2146.

[3] *Ling L ,Xiao Y ,Huang X , et al.* Design and Testing of Electric Drive System for Maize Precision Seeder[J].Agriculture,2024,**14**(10):1778-1778.

[4] *Wang Yanhong.* Uncovering the Secret: Agricultural Machinery Industry in Developed Countries in Europe and the United States [J]. Agricultural Machinery, 2018,(10): 36-38.
[5] *Nikolay Z ,Nikolay K ,Xiang Y H , et al*. Line laser based sensor for real-time seed counting and seed miss detection for precision planter[J].Optics and Laser Technology,2023,167
[6] *Jiaze S ,Yan Z ,Yuting Z , et al*. Precision Seeding Compensation and Positioning Based on Multisensors[J].Sensors,2022,**22**(19):7228-7228.
[7] *Xing H ,Wan Y ,Zhong P , et al*. Design and experimental analysis of real-time detection system for The seeding accuracy of rice pneumatic seed metering device based on the improved YOLOv5n[J].Computers and Electronics in Agriculture,2024,**227**(P2):109614-109614.
[8] *Kostic M, Rokic D, Radomirovic D, et al.* Corn seeding process fault cause analysis based on a theoretical and experimental approach[J]. Computers and Electronics in Agriculture, 2018,**151**:207-218.
[9] *Deng S ,Feng Y ,Cheng X , et al*. Disturbance analysis and seeding performance evaluation of a pneumatic-seed spoon interactive precision maize seed-metering device for plot planting[J].Biosystems Engineering,2024,**247**:221-240.
[10] *Bűdi K ,Bűdi A ,Tarcsi Á , et al.* Variable Rate Seeding and Accuracy of Within-Field Hybrid Switching in Maize (Zea mays L.)[J]. Agronomy,2025,**15**(3):718-718.
[11] *Weipeng Z ,Bo Z ,Shengbo G , et al*. Design and experiment of an intelligent testing bench for air-suction seed metering devices for small vegetable seeds[J].Biosystems Engineering,2024,**245**:84-95.
[12] *Pengfei Z ,Xiaojun G ,Yuan S , et al*. Investigation of seeding performance of a novel high-speed precision seed metering device based on numerical simulation and high-speed camera[J].Computers and Electronics in Agriculture,2024,**217**:108563-.
[13] *Bhushan B S ,R. R ,Abhay C , et al.* Designing and implementing a smart transplanting framework using programmable logic controller and photoelectric sensor[J].Energy Reports,2022,**8**(S9):430-444.
[14] *Jin Q, Lin K X, Yang S, et al.* Research and application of intelligent agricultural equipment technology abroad [J]. Agricultural Machinery and Supervision, 2020,(7): 32-33.
[15] *Ma C ,Zhao Z ,Chen X , et al*. Optimization of Seed-Receiving Mechanism in Belt-Driven Seed Guide Tube Based on High-Speed Videography Experiment[J].Agriculture,2025,**15**(2):174-174.
[16] *Gonçalves F M ,Ganancini G Z ,Paulo S J , et al.* Sensors installation position and its interference on the precision of monitoring maize sowing[J].Smart Agricultural Technology,2023,4.
[17] *Wang Song, Zhao Bin, Kuang Lihong, et al*. Research status and prospect of electric drive seeding technology [J]. Research in Agricultural Mechanization, 2022,**44**(12): 1-7 +21.
[18] *Xiaolong L ,Hongji H ,Wencheng W , et al*. Seed motion characteristics and seeding performance of a centralised seed metering system for rapeseed investigated by DEM simulation and bench testing[J].Biosystems Engineering,2021,**203**:22-33.
[19] *Cao Ye*. Design of Seed Metering Performance Detection System of Hole Seeder Based on Machine Vision [D]. Xinjiang: Tarim University, 2021.
[20] *Wang S ,Yi S ,Zhao B , et al*. Sowing Depth Monitoring System for High-Speed Precision Planters Based on Multi-Sensor Data Fusion[J].Sensors,2024,**24**(19):6331-6331.
[21] *Davut K ,Egidijus Š ,Ali A* .Design and Experiment of a Helicoidal Seed Tube to Improve Seed Distribution Uniformity of Seed Drills[J].Processes,2022,**10**(7):1271-1271.
[22] *Li Yanming, Qin Chengjin, et al*. Design and experiment of capacitance detection system for wheat sowing rate [J]. Journal of Agricultural Engineering, 2018,**34**(18): 51-58.
[23] *Li L ,Wu G ,Meng Z , et al*.Design of Positive Pressure Re-Acceleration Assisted Seeding Mechanism for Corn Based on CFD-EDEM Gas-Solid Coupling Simulation[J].Agriculture,2024,**14**(11):1927-1927.
[24] *Yang Shuo, Wang Xiu, x, et al.* Study on on-line monitoring of grain spacing and early warning system of missed sowing in precision sowing of maize [J]. Acta Agricultural Machinery, 2021,**52**(3): 17-24 +35.
[25] *Liu Y F, Lin J, Li B F, et al.* Design and test on seeding-hole of horizontal plate for corn precision planter[J]. Transactions of the Chinese Society of Agricultural Engineering (Transactions of the CSAE), 2017,**33**(8): 37-46.
[26] *He X N, Wang R Z, Yang Z A, et al.* Design and Experiment of Brush-Belt Type High-Speed Seed Guiding Device for Maize[J]. Transactions of the Chinese Society of Agricultural Engineering (Transactions of the CSAE), 2025,**41**(8): 17-27.